Biomass Conversion and Biorefinery (2024) 14:3385–3395
https://doi.org/10.1007/s13399-022-02586-y

ORIGINAL ARTICLE

Preparation of cellulose-PVA blended hydrogels for wound healing applications with controlled release of the antibacterial drug: an in vitro anticancer activity

P. Sankarganesh[1] · V. Parthasarathy[2] · A. Ganesh Kumar[3] · S. Ragu[4] · M. Saraniya[4] · N. Udayakumari[4] · R. Anbarasan[5]

Received: 13 December 2021 / Revised: 11 March 2022 / Accepted: 12 March 2022 / Published online: 6 April 2022

Abstract

Recently, extensive research works are going on hydrogel-based wound healing and drug release materials. In the present research work, PVA/cellulose hydrogel (PCH) membrane was prepared to assess its drug release activity against pathogens or microorganisms and cancer-causing Jurkat cells. The structure of the PVA/cellulose hydrogel was confirmed by FTIR and XRD. The morphology of the PCH membrane was assessed by SEM. The thermal stability of the PCH membrane was assessed by TGA. The –OH stretching appeared at 3366 cm^{-1} in the FTIR spectrum. The XRD confirmed the amorphous nature of the PVA/cellulose hydrogel membrane. The percentage residue that remained above 600 °C was higher for PCH membrane as compared with PVA. The wound dressing characteristics of the prepared PCH membrane were evaluated by performing various analyses such as swelling index, degradation, hemocompatibility, blood clot, and antibacterial drug delivery activity. The PCH membrane also showed a high water-absorbing potential. The hemocompatibility analysis proved that there was no marked level of hemolysis. The PCH membrane effectively inhibited the growth of pathogens or microorganisms and cancer-causing Jurkat cells by delivering the drugs at a controlled rate. In the present research work, the anticancer and antimicrobial properties of the PCH membrane were extensively studied. The drug release study of PVA/cellulose hydrogel was performed to analyze the drug release model and mechanism. The PCH membrane satisfied the important characteristics of ideal wound dressing materials.

Keywords PVA/cellulose hydrogel · Hemocompatible · Biodegradable · Antibacterial · Anticancer drug delivery

1 Introduction

Synthetic hydrogels have been employed as promising wound dress materials in wound care treatment for the last three decades. Hydrogels can be applied to a variety of wounds like burns and leg ulcers. However, the real benefits of hydrogels can be realized while using them in painful wounds since they reduce pains considerably due to their cooling and soothing effects. Hydrogels enhance the wound bed cellular activity by providing a moist environment around the wound. Hydrogel dressing enables wound healing faster than conventional dressing like lint, cotton, and gauze bandages due to its ability to maintain a warm and moist environment around the wound [1]. Hydrogels are having such potential characteristics, and the literature indicates that exploration of the same is not done so far in the biomedical field. This is the key idea of the present research work. The hydrogel is a hydrophilic polymer with a 3D network

✉ V. Parthasarathy
parthu0406@gmail.com

P. Sankarganesh
bilisankar@gmail.com

[1] Department of Food Technology, Hindustan Institute of Technology and Science, Padur-603103, Chennai, Tamil Nadu, India

[2] Department of Physics, Hindustan Institute of Technology and Science, Padur-603103, Chennai, Tamil Nadu, India

[3] Centre for Research & Development, Department of Microbiology, Hindustan College of Arts & Science, Padur-603103, Chennai, Tamil Nadu, India

[4] Department of Microbiology, Hindustan College of Arts & Science, Padur-603103, Chennai, Tamil Nadu, India

[5] Department of Chemical Engineering, National Taiwan University, Taipei 10617, Taiwan

that can retain a huge amount of water without any structural changes owing to its cross-linked polymer network. PVA is a synthetic, biocompatible, and hydrophilic polymer that can be used to prepare hydrogels by both physical and chemical techniques. PVA/cellulose-based hydrogels were reported by Mathilde et al. in the year 2021 [2]. PVA-based hydrogels have been considered as promising candidates for wound dressing applications. The physicochemical properties of PVA are significantly altered via blending either with natural or synthetic polymers. Therefore, PVA is blended with natural polymers to extend its biomedical applications. Cellulose is an abundant natural polymer that can be blended with PVA due to its insignificant toxicity, excellent biocompatibility, porous nature, and antibacterial property to prepare biopolymer-based hydrogels for wound healing applications. The PVA/bacterial cellulose composite was proposed as a bioactive wood dressing material for skin ulcer and burn treatment [3]. The PVA hydrogels were studied and also recommend as soft tissue substitutes by Mohamed et al. [4]. A highly transparent PVA hydrogel had been prepared to investigate its application in the development of artificial cornea [5]. The developed PVA/chitosan hydrogel was employed in treating osteochondral defects [6]. Anuj reviewed extensively the applications of PVA-based hydrogels in tissue engineering [7]. The antimicrobial activity of chestnut honey-based carboxymethyl cellulose hydrogel was evaluated against the *Escherichia coli* and *Staphylococcus aureus* by Park et al. [8]. The biomedical applications of biocompatible cellulose-based hydrogels had been reviewed extensively by Fu and his research team [9]. Rakhshaei et al. developed a carboxymethyl cellulose/ZnO-MCM-41 composite hydrogel with sustainable drug release properties for wound dressing [10]. Mao and his co-workers studied the wound healing and antibacterial activity of carboxymethyl cellulose hydrogel embedded with Ag/Ag@AgCl/ZnO nanostructure [11]. A gel matrix of PVA/polyethylene oxide/CMC blended with curcumin and aloe vera was prepared to develop antibacterial fabric dressings [12]. Lo et al. studied the full-thickness wound healing ability of cellulose-based hydrogel containing fibroblasts and keratinocytes cells [13]. Few reports on the natural polymer and PVA-based hydrogels cross-linked through a dialdehyde are available in the literature. Such hydrogels are biocompatible and cheaper with more biological activities. This motivated the authors to do the present research work.

Huang et al. studied xanthan-based film against *S. aureus* [14]. The antimicrobial potential of the baggase-cellulose hydrogel against *E. coli* was reported by Wang et al. [15]. Kamounand his research team [16] demonstrated the antibacterial activity of PVA-sodium alginate hydrogel membranes against *Staphylococcus pyogenes*, *Pseudomonas aeruginosa*, *Staphylococcus aureus*, and *Proteus vulgaris.* The antimicrobial potential of chitosan hydrogel was assessed against *S. aureus* and *E. coli* by Sudheeshkumar [17]. The poly(glutamic acid) and polylysine-glycidyl methacrylate hydrogels were used in wound healing and clinical antimicrobial therapy by Sun et al. [18]. The curcumin-loaded PVA/cellulose nanocrystals were examined against MCF-7 and Huh-7 cells by Yasmin and his co-workers [19]. There is no study on the drug delivery efficiency of PCH membrane against the *Staphylococcus aureus* (MCC strain-no: 2043) and *Pseudomonas aeruginosa* (MCC strain-no: 2082) in the open literature.

In the treatment of solid tumors, ionizing radiation is used along with usual medication. This treatment is an effective one in treating cancer. However, the normal tissues are severely damaged during the irradiation which leads to critical health complications. In 2017, a systematic review paper on impaired wound healing after radiation therapy was published by Jacobson et al. [20]. Deptula et al. [21] reported the wound healing complications in oncological patients. Gopinath and his research team [22] explained the dark side of wound healing. The post-operative wound complication in breast cancer was studied by Murthy et al. [23]. Payne and co-workers [24] reported the wound healing process in cancer patients. Our future research work will be on the wound healing study.

Curcumin finds wide applications in the biomedical field because of its biological activities. The drug delivery activity of curcumin-loaded chitosan was reported in the literature [25]. In 2019, Mahmoud et al. [26] reported the drug release kinetics of curcumin. The curcumin-loaded polymeric micro-particulate system was developed by Dana et al. [27]. Lanmei et al. [28] published a review article on the curcumin delivery system. Release kinetics and mechanism of curcumin-loaded cockle shell were reported by Maryam et al. [29]. Streptomycin has been used as an antibiotic to treat bacterial infections. The antibacterial study of streptomycin-loaded chitosan was reported by Samer and co-workers [30]. Kailash et al. [31] reported the sustainable release of streptomycin from poly(caprolactone) surface. In the present work, curcumin and streptomycin were used to improve the biological activity of hydrogels. The drug release activity of curcumin-loaded PVA/cellulose hydrogel against Jurkat cells is also not yet reported so far. Hence, the present investigation aims to evaluate the drug delivery efficiency of the PCH membrane against pus-inducing microbes and cancer cell lines.

2 Experimental

2.1 Chemicals

PVA (Mw-1,50,000 g/mol), glutaraldehyde (50% solution), curcumin, streptomycin, and Cellulose powder were

Scheme 1 Synthesis of glutaraldehyde-mediated PVA and cellulose-based hydrogel

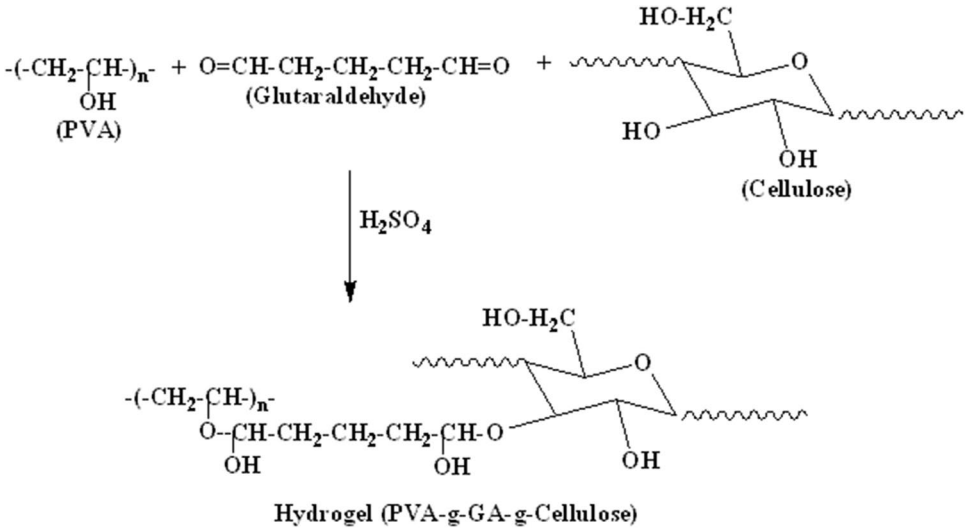

purchased from Sigma Aldrich Chemicals, USA. The washing and solution preparation was carried out using double distilled water.

2.2 Fabrication of PVA/cellulose hydrogel

Poly (vinyl alcohol)/cellulose hydrogel membrane was fabricated by the casting method [25]. In brief, 1 g of PVA was completely dissolved in 10 mL of distilled water at 95 °C under stirring. Then, the cellulose (250 mg) was separately dissolved in 10 mL of distilled water. Furthermore, it was mixed with aqueous PVA. During the mixing process, there was a formation of inter- and intra-molecular hydrogen bonding between the –OH group of PVA and cellulose. This led to the simple blending process. Then, 2 drops of Con. H_2SO_4 were slowly added to the PVA/cellulose solution followed by the addition of 1.4 mL of glutaraldehyde. The final hydrogel was dried in a hot air oven at 50 °C for 60–70 min. The reaction is given in Scheme 1.

2.3 Physicochemical analysis

The presence of functional groups in the prepared samples was confirmed by recording FTIR spectra (Shimadzu 8400 S, Japan) in the range of 400 to 4000 cm^{-1}. Two milligram of the sample was mixed with 200 mg of spectral grade KBr and made into a disc under the pressure of 7 tons. X-ray diffraction study was performed using Brucker K 8600 instrument in the 2θ range of 2 to 80° with the scanning speed of 2°/min. The TGA of the samples was examined using TG/DTA 6200 thermal analyzer in an air atmosphere at the heating rate of 10 °C min^{-1} from 30 to 700 °C [32, 33]. The surface morphology of the polymeric material was analyzed with the help of SEM instrument, JSM 6300, JEOL model, USA.

2.4 In vitro biodegradation level

The biodegradation potential was analyzed for the prepared PCH membrane [34]. For this analysis, PVA/cellulose hydrogel was cut into small pieces and incubated in the phosphate buffer (pH 7.4) solution containing lysozyme (0.2%) for about 7 h. Meantime, the samples were taken out of the buffer solution at a regular interval of time and washed thoroughly with deionized water. Then, the weight of the samples was measured after drying them properly. The degradation rate (S%) was determined by using the following equation:

$$Degradation\ rate(S\%) = \frac{W_0 - W_t}{W_0} \times 100 \quad (1)$$

where W_0 is the initial weight and W_t is the final weight.

2.5 Swelling index

The swelling behavior of the hydrogel membrane was examined to assess its water retention potential [35]. In brief, the pre-weighted hydrogel pieces (4 cm^2) were soaked in phosphate buffer (pH-7.4) at room temperature. Then, the soaked samples were taken out with the aid of blunt forceps at a regular interval of 5 min. Afterwards, they were blotted to remove the excess fluid. The weight of the samples was measured using an electronic balance and the swelling index (SI) was calculated by using the following equation:

$$Swelling\ index(SI) = \frac{W_2 - W_1}{W_1} \times 100 \quad (2)$$

where SI is the swelling index of the hydrogel at equilibrium, W_1 is the initial weight, and W_2 is the final weight

of the samples at equilibrium water absorption. The average value of SI was estimated by repeating the experiments thrice.

2.6 Moisture loss capacity

In brief, the PVA/cellulose hydrogel was cut into small strips of dimension about 20 × 20 mm to carry out moisture loss analysis [36]. The hydrogel strips were weighed before placing them in a desiccator. The weight of the samples was estimated for every 1 h until attained a constant weight. The moisture loss was evaluated by determining the difference between the initial and final weight of the samples.

2.7 Hemolysis analysis

Hemolysis gives an insight into the damages in the erythrocytic membranes (red blood cells). It can be identified by measuring the release of hemoglobin levels in the blood plasma. The hemolytic analysis evaluates an in vitro hemolytic potential of the prepared PVA-cellulose hydrogel. The procedure for this analysis is discussed here. The dry PVA/cellulose hydrogel was equilibrated in the saline solution for 24 h at 37 °C ± 0.5 °C. Then, the human ACD blood (0.25) was placed on the wet hydrogel. After 20 min, 2.0 mL of saline solution was added to the surface of the hydrogel. Then, the sample was incubated at 37 °C ± 0.5 °C for 60 min. The positive control was prepared by adding 0.25 mL of the human ACD blood in 2 mL of sterile distilled water. The saline solution was used as a negative control. The incubated samples were collected to record the optical density values at 545 nm [34]. The hemolytic percentage was calculated as follows:

$$Hemolysis(\%) = \frac{absorbance\ of\ test\ sample - absorbance\ of\ negative\ control}{absorbance\ of\ positive\ control - absorbance\ of\ negative\ control} \times 100 \quad (3)$$

The absorbance values for positive and negative controls are 1.25 and 0.010 respectively.

2.8 Blood clot analysis

The anti-thrombogenic property of PVA-cellulose hydrogel was evaluated by carrying out the blood clot analysis [34]. In brief, PVA/cellulose hydrogel was equilibrated in saline solution at 37 °C ± 0.5 °C for 24 h. 0.5 mL of acid citrate dextrose (ACD) was placed on the wet hydrogel followed by the addition of 0.03 mL of the calcium chloride solution (4 mol/L) to initiate thrombus formation (blood clot). This process was further terminated by adding 4.0 mL of deionized water. Afterwards, the sample was soaked in deionized water for 10 min at room temperature to separate the obtained thrombus. Then, the thrombus was kept in 36% v/v formaldehyde solution (2.0 mL) for 10 min and placed in deionized water for 10 min. Finally, the sample was completely dried to measure its weight. The same procedure was repeated to conclude the formation of a thrombus on the glass surface.

2.9 Antimicrobial drug delivery analysis

Five different concentrations of Streptomycin (10–50 mg) were separately loaded onto PVA/cellulose hydrogel to investigate their antimicrobial drug release activity against pus-inducing microbes such as *Staphylococcus aureus* (MCC strain-no: 2043) and *Pseudomonas aeruginosa* (MCC strain-no: 2082) by disc diffusion assay according to Clinical and Laboratory Standard Institute (CLSI) guidelines [37, 38].

2.10 In vitro cytotoxicity analysis

MTT [3–4(4,5-dimethylthiazol-2-yl)-2,5-diphenyltetrazolium bromide] assay is used to measure the cell viability, proliferation, and cytotoxicity under in vitro conditions. This study was carried out to investigate the effect of curcumin-loaded PVA/Cellulose hydrogel against the immortalized T-lymphocyte Jurkat cells [39].

2.11 Drug delivery study

The drug release model and mechanism were determined by carrying out the drug release analysis. The drug release activity was performed in a buffer solution for PVA/cellulose hydrogel by using the standard procedure [31]. 0.50 g of PCH membrane was made as a disc by applying pressure (7 tons). The drug release potential of the PCH membrane was assessed by suspending the disc in 500 mL of PBS buffer solution at gastric pH. A UV–Visible spectrum was captured to follow the drug release kinetics. The percentage cumulative drug release (CDR) was computed using Eq. (4):

$$\%CDR = \frac{(\text{weight of standard}) \times (\text{sample absorbance}) \times (\text{sample dilution}) \times (\text{potency standard})}{(\text{standard dilution}) \times (\text{standard absorbance}) \times (\text{label claim})} \quad (4)$$

The various drug release models were employed to study the drug release potential of the PCH membrane. The plots of (% CDR) versus time and log(% drug remaining) versus time were drawn to study the Zeroth and first-order drug release activities of PCH membrane respectively. The plots of log(% CDR) versus log(time) (Korsmeyer-Peppas model), (% drug remaining)$^{1/3}$ versus time (Hixson-Crowell model), and % CDR versus (time)$^{1/2}$ (Higuchi model) were also drawn to study the drug release profile of PCH membrane. The drug release model and mechanism were concluded from the n value of the Korsmeyer-Peppas plot and the max R^2 value.

3 Results and discussion

3.1 FTIR study

The structure of PVA, cellulose, and PVA/cellulose hydrogel was examined by analyzing their FTIR spectra. The FTIR spectrum of PVA is illustrated in Fig. 1a. The hydroxyl (O–H) group of PVA is assigned at 3366 cm^{-1}. The C-H asymmetric stretching is observed in the wavenumber region of 2930 cm^{-1}. The carbonyl (C = O) stretching mode of the ester group of PVA is observed at 1731 cm^{-1} [40]. The peak at 1414 cm^{-1} and 1368 cm^{-1} are attributed to the –CH_2 bending and wagging modes respectively. A peak at 1575 cm^{-1} is linked to C-H wagging vibration. The characteristic stretching modes of C–O–C and –CH_2 of pristine PVA are noticed at 1080 cm^{-1} and 833 cm^{-1} respectively. Figure 1b depicts the FTIR spectrum of pristine cellulose. A peak at 3303 cm^{-1} is related to hydroxyl (O–H) stretching vibrations of cellulose. The C-H symmetric deformation (1363 cm^{-1}), C-O anti-symmetric bridge stretching (1157 cm^{-1}), and C–O–C pyranose ring skeletal vibrations (1030 cm^{-1}) are attributed to the structure of cellulose. The β-glucosidal linkage of sugar units is seen at 897 cm^{-1}. The FTIR spectrum of PVA-cellulose hydrogel is shown in Fig. 1c. The interaction of cellulose with PVA occurs through the strong linkage between the hydroxyl groups of cellulose and PVA. The peak associated with the O–H group of PVA-cellulose hydrogel seems to be broader as compared with the O–H group of PVA due to the strong intermolecular bond formation between cellulose and PVA.

3.2 XRD analysis

The structural analysis was carried out for the prepared samples using XRD. The XRD profile of pure PVA is depicted in Fig. 2a. A peak at 19.8° is related to the (101) crystal plane of PVA, which confirms the semi-crystalline nature of PVA [41]. The XRD pattern of cellulose exhibits three well distinct diffraction peaks, at 2θ = 16.4, 22.8, and 34.2° as shown in Fig. 2b. These diffraction peaks arise due to the reflection from the different crystal planes of cellulose such as (010), (002), and (040). Figure 3c represents the XRD pattern of PVA/cellulose hydrogel [42]. The characteristic peaks of PVA and cellulose do not appear in the XRD pattern of PVA/cellulose hydrogel. The structure of PVA and cellulose is greatly altered after the interaction of cellulose with the PVA matrix. The XRD profile revealed the amorphous nature of PVA/cellulose hydrogel [43].

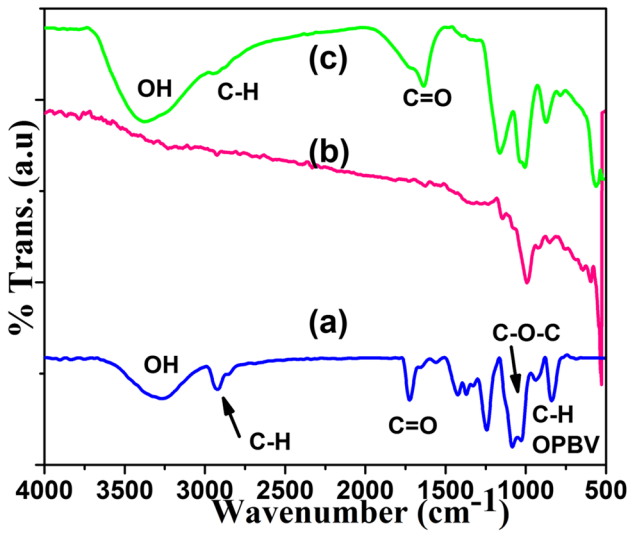

Fig. 1 FTIR spectra of **a** pure PVA, **b** cellulose, and **c** PVA/cellulose hydrogel

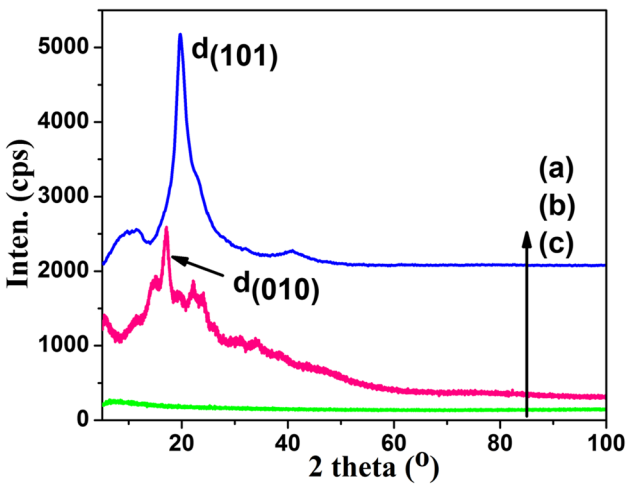

Fig. 2 XRD patterns of **a** Pure PVA, **b** cellulose, and **c** PVA/cellulose hydrogel

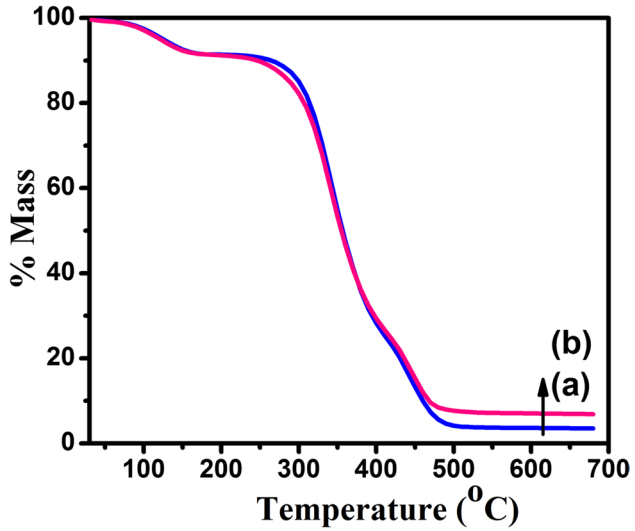

Fig. 3 TG thermograms of **a** pure PVA and **b** PVA/cellulose hydrogel

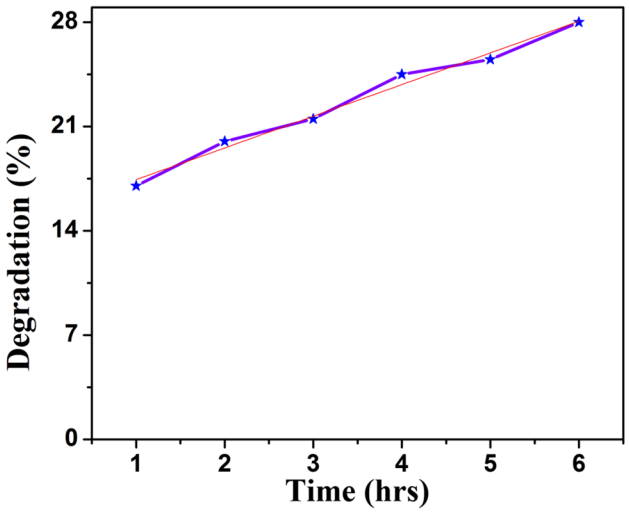

Fig. 4 In vitro biodegradation(S%) ratio of PVA/cellulose hydrogel

3.3 TGA analysis

The thermal stability of PVA and PVA/cellulose hydrogel was assessed using TGA. The TGA gives additional information about the thermal degradation temperature of the material and it is independent of the processing temperature. The TG thermograms of PVA and PVA/cellulose hydrogel are shown in Fig. 3a and b. All the thermograms exhibit two-step degradation processes. The first step degradation extends up to 255 °C for both pure PVA and PVA/cellulose hydrogel, which is attributed to the removable of physisorbed and chemisorbed water molecules. The major weight loss associated with the second-step degradation process of pure PVA is due to the degradation of the PVA backbone. The second-step degradation starts around 265 °C which further extends up to 484 °C by leaving only 3% of weight residue above 500 °C for pure PVA. However, the second-step degradation occurs at 256 °C which extends up to 478 °C by leaving 8% of weight residue above 500 °C for PVA/cellulose hydrogel. The % weight residue remained above 500 °C is higher for PVA/cellulose hydrogel as compared with PVA. Hence, the PVA/cellulose hydrogel is thermally stable at a higher temperature as compared with pure PVA.

3.4 In vitro biodegradation

Figure 4 describes an in vitro biodegradation (S %) potential of PVA/cellulose hydrogel. It was observed that there was a slower rate of weight loss during the period of 7 h while incubating PVA/cellulose hydrogel in PBS solution containing 0.2% of lysozyme. The weight loss of the PVA/cellulose hydrogel membrane proved its degradation potential in PBS solution. This can be attributed to the lower accessibility of the lysozyme that interacts with PVA/cellulose hydrogel. When compared with neat PVA, the PVA/cellulose system exhibited excellent biodegradation results (not reported here). This increased enzymatic stability is one of the significant important parameters for dressing materials [44].

3.5 Swelling index (SI)

The formation of intermolecular bonds between the hydroxyl group of PVA and functional groups of cellulose generally influences the swelling index of PVA/cellulose hydrogel [45]. The swelling index values of PVA/cellulose hydrogel are presented in Fig. 5. The SI of PVA-cellulose hydrogel was about 50% in 10 min. Then, it increased to 110% within 40 min. Afterwards, it reached a maximum of 200% in 70 min. This proved the slow water absorption

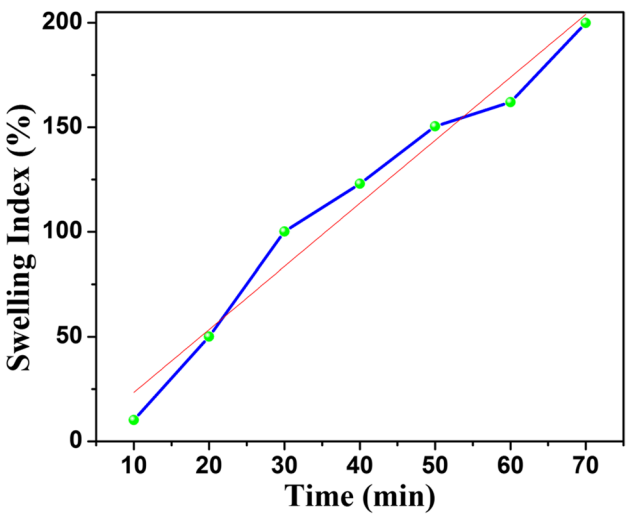

Fig. 5 Swelling index analysis of PVA/cellulose hydrogel

behavior of the PCH membrane. The SI of PVA/cellulose hydrogel showed an equilibrium swelling after the 7th hour of incubation in pure water. It proved an excellent water absorbing potential of PVA/cellulose hydrogel. It is one of the desired properties for wound dressing applications. The obtained clinical results proved that the polymeric hydrogels offer a moist environment around the wound site to empower the healing process by controlling damaged skin from cellular dehydration and angiogenesis. Hence, this polymer hydrogel can be considered a potential candidate for wound dressing applications. When compared with the neat PVA, the swelling index of PVA/cellulose hydrogel exhibited excellent results due to the availability of more OH groups and porous structure.

3.6 Moisture loss study

The water dehydration level of PVA/Cellulose hydrogel was evaluated at different time intervals by measuring its weight. The results of moisture loss analysis indicated a poor loss of water molecules by PVA/cellulose hydrogel under desiccation conditions. This proved that PVA/cellulose hydrogel can retain high moisture content in its dense polymeric network for a long time (Fig. 6). The moisture loss of PVA/cellulose hydrogel is higher than the neat PVA system. The results are not shown here. The possible reasons are explained above.

3.7 Hemocompatibility and blood clot analysis

The PVA/cellulose hydrogel exhibited 4.03% of hemolysis (Fig. 7a). It proved that there was no marked level

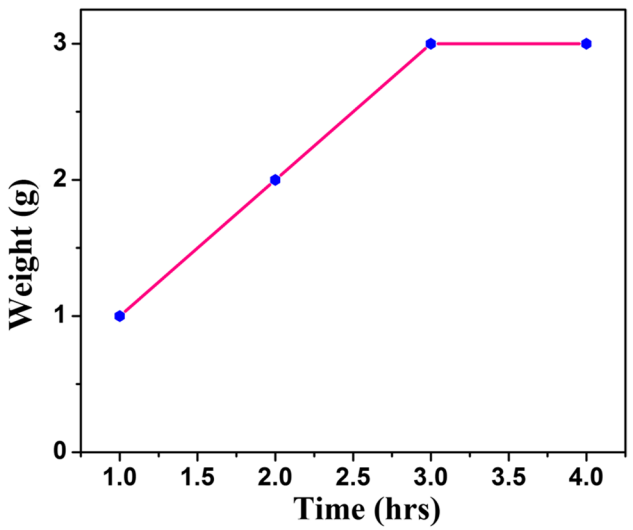

Fig. 6 Water loss analysis of PVA/cellulose hydrogel

Fig. 7 **a** Hemolysis analysis, **b** blood clot analysis of PVA/cellulose hydrogel

of erythrocytic membrane damage by the prepared PCH membrane. Moreover, it is biocompatible with red blood cells (RBC). Therefore, the prepared PCH membrane is more suitable for wound dressing applications.

3.8 Blood clot analysis

The anti-thrombogenic potential of the PVA/cellulose hydrogel was examined by comparing the thrombus formation (blood clot) on the glass with the hydrogel. The weight of the glass was increased by 1.5%, whereas it was only 0.5% for PVA/cellulose hydrogel after thrombus formation (Fig. 7b). Comparatively, PVA/cellulose hydrogel recorded a low level of fibrin clot deposition. It indicated that PVA/cellulose did not induce any high level of thrombus formation during this analysis. Therefore, the prepared PVA/cellulose hydrogel is more suitable for wound dressing material as it possesses important characteristics for wound dressing applications [46].

3.9 Drug delivery efficacy against pus-inducing microbes

In this study, Streptomycin-loaded PVA/cellulose hydrogel was assessed to evaluate the antimicrobial activity against *S. aureus* (MCC No: 2043) and *P. aeruginosa* (MCC No: 2082) by disk diffusion method. The diameter of the inhibition

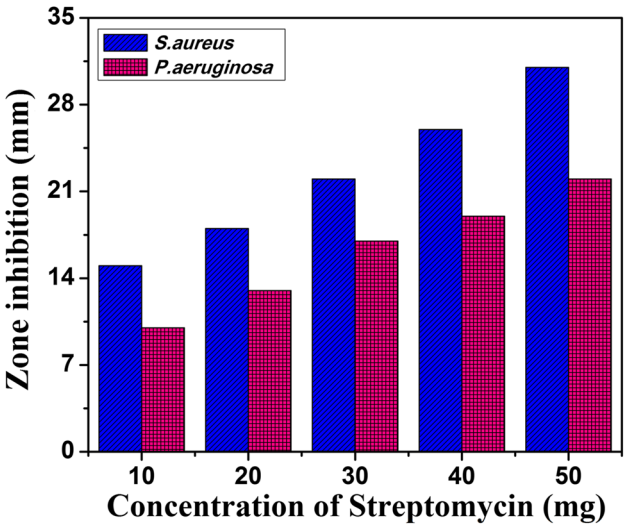

Fig. 8 Streptomycin drug delivery potential of PVA/cellulose hydrogel against pathogenic *S. aureus* (MCC strain no: 2043) and *P. aeruginosa* (MCC strain no: 2082)

zone was measured after 24 h. It was noticed that the drug-loaded PVA/cellulose hydrogel was effectively released the Streptomycin against *S. aurues* and *P. aeruginosa*. The diameter of the inhibition zone was increased while increasing the concentration of the Streptomycin as shown in Fig. 8. The *S. aureus* exhibited a greater inhibition zone as compared with *P. aeruginosa* for streptomycin. This activity is supporting the swelling index and moisture loss capacity of PVA/cellulose hydrogel. This is in accordance with the literature report [47]. The variation in the zone diameter is mainly associated with the antibiotic response against organisms. These results suggested an excellent drug delivery potential of PVA/cellulose hydrogel against pathogenic microorganisms. The reason behind the controlled release of the drug may be due to intermolecular interactions between the antibiotic and polymer hydrogel.

3.10 Drug delivery efficacy against cancer cells (in vitro)

The cytotoxicity analysis of the curcumin-loaded PVA/cellulose hydrogel is presented here. Almost all the cancer cells (91.6%) had been identified as non-viable after 7 days of contact with the PVA/cellulose hydrogel (Fig. 9). In the control sample (without curcumin), the Jurkat cell's growth was not affected even after the 7th day of incubation. However, the growth of cancer cells was retarded gradually while exposing the cells to 1% curcumin-loaded PVA/cellulose hydrogel. The PCH membrane effectively delivered curcumin against Jurkat cells. It was noticed that the growth of the Jurkat cells was reduced to 14.2% on the third day of incubation. In the meantime, curcumin is acting as a bio-marker. Hence, the extra bio-marker was not added in this work. Moreover, the alive Jurkat cells were only 4.8% on the seventh day of incubation (Table 1).

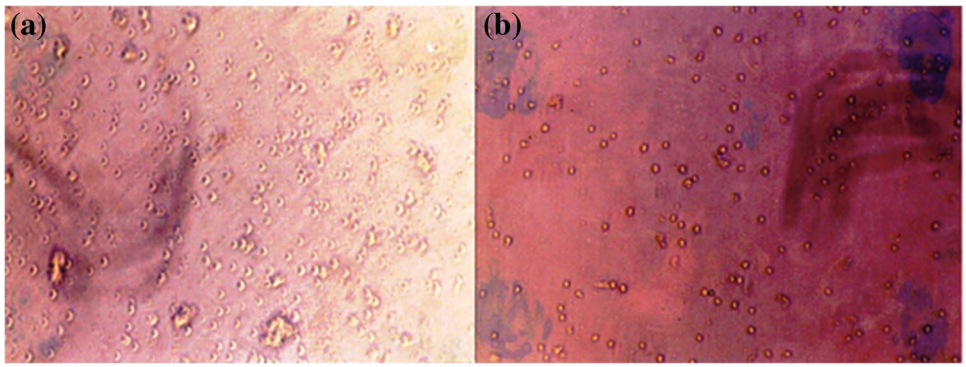

Fig. 9 **a** Curcumin-loaded PVA/cellulose hydrogel and **b** PVA/cellulose hydrogel (without curcumin)

Table 1 Curcumin delivery efficiency of PVA/Cellulose hydrogel against Jurkat cells

System	3rd day of cell culture			5th day of cell culture			7th day of cell culture		
	All cells (%)	Alive cells (%)	Non-viable cells (%)	All cells (%)	Alive cells (%)	Non-viable cells (%)	All cells (%)	Alive cells (%)	Non-viable cells (%)
Control sample	90.2	95.2	4.5	80.2	88.6	9.1	78.2	98.2	0.80
PVA/cellulose hydrogel treated with curcumin	77.1	14.2	82.3	64.2	4.8	91.2	60.2	7.2	91.6

However, the number of alive cells increased after the seventh day. It was concluded that the PCH membrane effectively released curcumin only up to the 5th day. Hence, the drug-loaded PVA/cellulose hydrogel membrane can be applied to the wounds of cancer patients. The optical images were recorded without adding a marker. When compared with the wound of the normal person, it would be clearer. This is because of the damaged cancer cells and improperly aligned proteins.

3.11 SEM analysis

The surface morphology of pristine PVA (Fig. 10a), cellulose (Fig. 10b), and PVA/cellulose hydrogel (Fig. 10c) are presented here for the sake of comparison. The cellulose showed the fiber-like morphology, whereas the hydrogel exhibited the cage-like morphology. The hydrogel exhibited an entirely different morphology as compared with pristine PVA and cellulose. Thus the SEM confirmed the formation of a hydrogel.

3.12 Drug release study

The drug release activity of the PVA/cellulose hydrogel system was investigated by capturing the UV–Visible spectra (not given here) at a regular interval of 1 min. There was an increase in OD value at 351 nm while increasing the concentration of Streptomycin. It was found that the First-order model exhibited the maximum R^2 value [Fig. 11a]. Furthermore, the Korsmeyer-Peppas (K-P) model was drawn with a slope value of 0.80 [Fig. 11b]. The slope value confirmed the

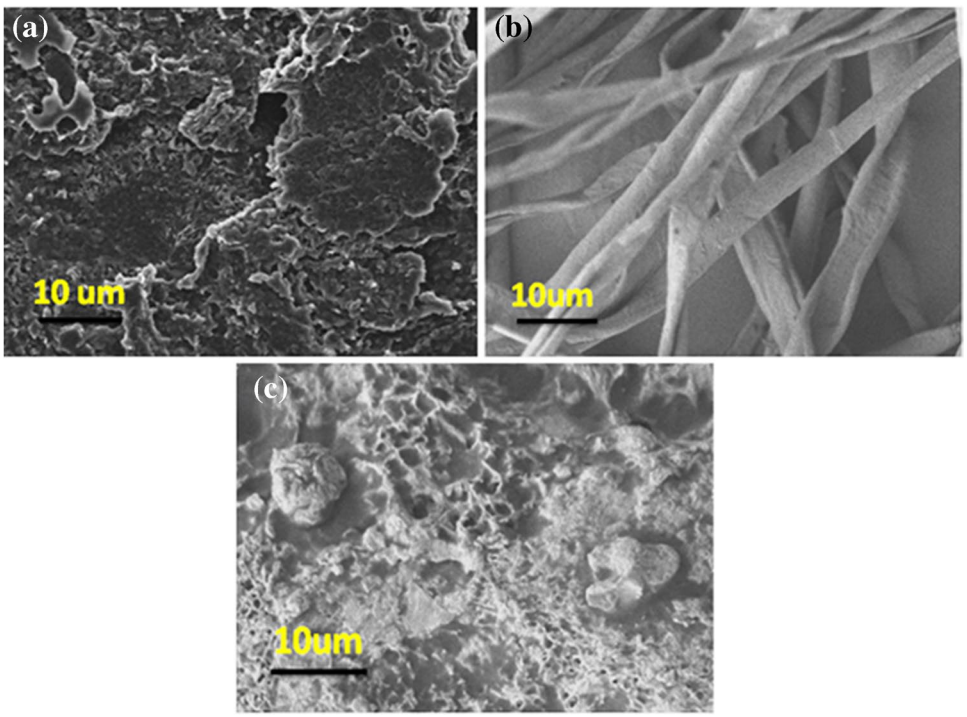

Fig. 10 SEM image of **a** neat PVA, **b** cellulose, **c** PVA/cellulose hydrogel

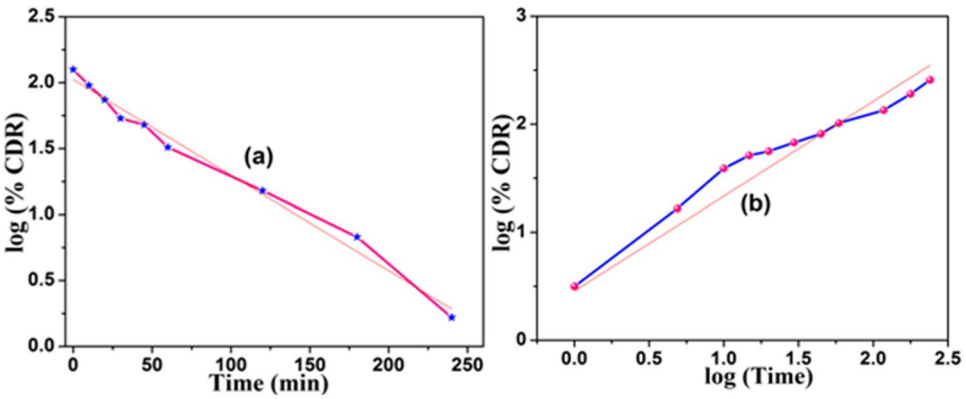

Fig. 11 **a** First-order model plot, **b** K-P model plot

non-Fickian drug transportation mechanism (i.e.) release of streptomycin from the PVA/cellulose hydrogel backbone. In this work, the release of the drug took place from the hydrogel backbone by breaking the hydrogen bond (i.e.) breaking of inter and intra-molecular hydrogen bonding. This depends on the availability of a number of hydroxyl groups. The drug release data revealed an excellent drug release activity for the prepared polymeric hydrogel system. The results are in accordance with the literature report [31].

4 Conclusions

The PCH membrane was successfully prepared by the casting technique. The interaction of cellulose with PVA occurred through the strong linkage between the hydroxyl groups (~ 3600 cm^{-1}) of cellulose and PVA. It was further confirmed by FTIR. The XRD of the PCH membrane showed amorphous nature. The PCH membrane exhibited two-step degradation processes in TGA and its T_d was low as compared with the reported literature. The PVA/cellulose hydrogel showed a cage-like surface morphology in the SEM micrographs. The prepared PCH membrane exhibited a good moisture-retaining ability, biodegradability, and biocompatibility as compared with the literature reports. The PVA/cellulose hydrogel effectively delivered the Streptomycin (antibiotic) against pus-inducing pathogens. The curcumin-loaded PVA/cellulose hydrogel effectively reduced the growth of cancer-causing Jurkat cells to 14.2% on the 3rd day and left only 4.8% of alive Jurkat cells on the 7th day of inhibition. PVA/cellulose hydrogel recorded a low level of fibrin clot deposition which proved a very low thrombus formation. There was no erythrocytic membrane damage by the prepared PVA/cellulose hydrogel. The drug release followed the non-Fickian drug transportation mechanism. The PVA/cellulose hydrogel can be used as promising dressing materials for different types of wounds including cancer-treated wounds. In the future, my research team will thoroughly study the wound healing complications in cancer patients. This will be a new breakthrough in the oncology field.

Declarations

Conflict of interest The authors declare no competing interests.

References

1. Santiago C, Abigail KG, Hector LH, Doreen C, Anthony CY, Lyndsay MS, Eric AA (2021) Translaional applications of hydrogels. Chem Rev 121:11385–11457. https://doi.org/10.1021/acs.chemrev.0c01177
2. Mathilde S, Claude-Olivier S, Erwann G, Christophe E, Frédéric D (2021) Cellulosic/polyvinyl alcohol composite hydrogel: synthesis, characterization and applications in tissue engineering. Polymers 13:3598. https://doi.org/10.3390/polym13203598
3. Osorio M, Velásquez-Cock J, Restrepo LM, Zuluaga R, Gañán P, Rojas OJ, Ortiz-Trujillo I, Castro C (2017) Bioactive 3D-shaped wound dressings synthesized from bacterial cellulose: effect on cell adhesion of polyvinyl alcohol integrated in situ. Int J Polym Sci 3728485.https://doi.org/10.1155/2017/3728485
4. Mohamed SBH, Arun G, Basma YA, Swati S (2018) Synthesis of PVA/PVP based hydrogel for biomedical applications: a review. Energy Sources, Part A: Recover Util Environ Eff 40(20):2388–2393. https://doi.org/10.1080/15567036.2018.1495786
5. Hou Y, Chen C, Liu K, Tu Y, Zhang L, Li Y (2015) Preparation of PVA hydrogel with high transparency and investigation of its transparent mechanism. RSC Adv 5:24023–24030. https://doi.org/10.1039/C5RA01280E
6. Peng L, Zhou Y, Lu Y, Zhu W, Yusheng L, Chen K, Zhang G, Xu J, Deng Z, Wang D (2019) Characterization of a novel polyvinyl alcohol/chitosan porous hydrogel combined with bone marrow mesenchymal stem cells and its application in articular cartilage repair. BMC Musculoskelet Disord 20:257. https://doi.org/10.1186/s12891-019-2644-7
7. Anuj K, Han SS (2017) PVA-based hydrogel for tissue engineering: a review. Int J Poly Mater Poly Biomater 66(4):159–182. https://doi.org/10.1080/00914037.2016.1190930
8. Park J, An SJ, Jeong S, Gwon H, Lim YM, Chang Y (2017) Chestnut honey impregnated carboxymethyl cellulose hydrogel for diabetic ulcer healing. Polymers (Basel) 9(7):248. https://doi.org/10.3390/polym9070248
9. Fu LH, Qi C, Ma MG, Wan P (2018) Multifunctional cellulose-based hydrogels for biomedical applications. J Mater Chem B 7(10):1541–1562. https://doi.org/10.1039/C8TB02331J
10. Rakhshaei R, Namazi H (2017) A potential bioactive wound dressing based on carboxymethyl cellulose/ZnO impregnated MCM-41 nanocomposite hydrogel. Mater Sci Eng C 73:456–464. https://doi.org/10.1016/j.msec.2016.12.097
11. Mao C, Xiang Y, Liu X, Cui Z, Yang X, Yeung KWK, Pan H, Wang X, Chu PK, Wu S (2017) Photo-inspired antibacterial activity and wound healing acceleration by hydrogel embedded with Ag/Ag@AgCl/ZnO nanostructures. ACS Nano 11:9010–9021. https://doi.org/10.1021/acsnano.7b03513
12. Alven S, Khwaza V, Oyedeji OO, Aderibigbe BA (2021) Polymer based scaffolds loaded with Aloe vera extract for the treatment of wounds. Pharmaceutics 13:961. https://doi.org/10.3390/pharmaceutics13070961
13. Loh E, Mohamad N, Fauzi M, Ng M, Ng S (2018) Development of a bacterial cellulose-based hydrogel cell carrier containing keratinocytes and fibroblasts for full-thickness wound healing. Sci Rep 8(1):2875. https://doi.org/10.1038/s41598-018-21174-7
14. Huang J, Ren J, Chen G, Deng Y, Wang G, Wu X (2017) Evaluation of the xanthan-based film incorporated with silver nanoparticles for potential application in the nonhealing infectious wound. J Nanomat 6802397.https://doi.org/10.1155/2017/6802397
15. Wang Y, Zhao X, Li X, Cai P (2019) Green based antimicrobial hydrogels prepared from bagasse cellulose as 3D-scaffolds for wound dressing. Polymer 11(11):1846. https://doi.org/10.3390/polym11111846
16. Kamoun E, Kenawy E, Tamer T, El-Meligy M, Eldin M (2015) Poly (vinyl alcohol)-alginate physically crosslinked hydrogel membranes for wound dressing applications: characterization and bio-evaluation. Arab J Chem 8(1):38–47. https://doi.org/10.1016/j.arabjc.2013.12.003

17. Sudheeshkumar P, Lakshmanan V, Biswas R, Shantikumar V, Jayakumar R (2012) Synthesis and biological evaluation of chitin hydrogel/nano ZnO composite bandage as antibacterial wound dressing. J Biomed Nanotech 8(6):891–900. https://doi.org/10.1166/jbn.2012.1461
18. Sun A, He X, Li L, Li T, Liu Q, Zhou X, Ji X, Qian Z (2020) An injectable photopolymerized hydrogel with antimicrobial and biocompatible properties for infection skin regeneration, NPG Asia Nanomat 12(25). https://doi.org/10.1038/s41427-020—0206-y
19. Yasmein H, Loutfy S, Kamoun E, El-Moslamy S, Radwanv E, Elbehairi S (2021) Enhanced anti-cancer activity by localized delivery of curcumin form PVA/CNCs hydrogel membranes: preparation and in vitro bioevaluation. Int J Biol Macromol 170:107–122. https://doi.org/10.1016/j.ijbiomac.2020.12.133
20. Jacobson L, Johnson MB, Wong AK (2017) Impaired wound healing after radiation therapy: a systematic review of pathogenesis and treatment. JPRAS 13:92–105. https://doi.org/10.1016/j.jpras.2017.04.001
21. Deptula M, Wardowska A, Pikula M (2019) Wound healing complications in oncological patients: perspectives for cellular therapy. Postepy Dermatol Alergol 36:139–146. https://doi.org/10.5114/ada.2018.72585
22. Gopinath M, Shan S, Sambath P (2018) Cancer; the dark side of wound healing. FEBS 285:4516–4534. https://doi.org/10.1111/febs.14586
23. Murthy B, Thomson C, Dodwell D (2007) Post operative wound complications and systemic recurrence in breast cancer. Br J Cancer 97:1211–1217. https://doi.org/10.1038/sj.bjc.6604004
24. Payne WG, Naidu DK, Wheeler CK, Robson MC (2008) Wound healing in patient with cancer. Eplasty 8:e9
25. Antony AS, Ujjala B, Sheryl AP, Kumar C (2018) Synthesis of curcumin loaded polymeric nanoparticles from crab shell derived chitosan for drug delivery. Infor Med Unloc 10:159–182. https://doi.org/10.1016/j.imu.2017.12.010
26. Mahmoud H, Kamil E, Cyril JFH, Elmira AT, Michael L (2019) Preparation, characterization ad release kinetics of chitosan coated nanoliposomes encapsulating curcumin in simulated environments. Molecules 24:2023. https://doi.org/10.3390/molecules24102023
27. Dana T, Lucia RT, Ioan T, Alina P (2020) Development of curcumin loaded polymeric microparticulate oral drug delivery system for colon targeting by quality-by-design approach. Pharmaceutics 12:1027. https://doi.org/10.3390/pharmaceutics12111027
28. Lanmei L, Xiamei Z, Chao P, Yumeng W (2020) Review of curcumin physicochemical targeting delivery system. Int J Nanomed 15:9799–9821
29. Maryam M, Kabeer A, Samaila MC, Zuki AZ (2019) Evaluation of invitro release kinetics and mechanism of curcumin loaded cockle shell derived calcium carbonate nanoaparticles. Biomed Res Ther 6:3518–3540
30. Samer HHA, Mohamed EE, Thomas JW (2014) Synthesis, characterizatioin and release and antibacterial studies of novel streptomycine /chitosan magnetic nanoantibiotic. Int J Nanomed 9:549–557
31. Kailash S, Meenarathi B, Parthaarathy V, Anbarasan R (2020) Conjugated hydrophobic and hydrophilic blocks through a drug moiety as a leading macromolecular system for sustainable drug delivery. J Polym Res 27:355. https://doi.org/10.1007/s10965-020-02302-2
32. Park Y, MyungilYo U, Shin J, sumin Ha, Dukeun Kim, Min HaengHeo, Junghyo Nah, YoongAhm Kim, Jae Hun seol, (2019) thermal conductivity enhancement in electrospun poly(vinyl alcohol) and poly(vinyl alcohol)/cellulose nanocrystal composite nanofibers. Sci Rep 9:3026. https://doi.org/10.1038/s41598-019-39825-8
33. Peng N, Wang Y, Ye Q, Liang L, An Y, Li Q, Chang C (2016) Biocompatible cellulose-based superabsorbent hydrogels with antimicrobial activity. Carbohydr Polym 137:59–64. https://doi.org/10.1016/j.carbpol.2015.10.057
34. Momin M, Kurhade S, Khanekar P, Mhatre S (2016) Novel biodegradable hydrogel sponge containing curcumin and honey for wound healing. J Wound Care 25(6):364–372. https://doi.org/10.12968/jowc.2016.25.6.364
35. Noori S, Kokabi M, Hassan ZM (2018) Poly(vinyl alcohol)/chitosan/honey/clay responsive nanocomposite hydrogel wound dressing. J Appl Polym Sci 135(21):46311. https://doi.org/10.1002/app.46311
36. Ahamed S, Manzoor K, Purwar R, lkram S, (2020) Morphological and swelling potential evaluation of *Moringa oleifera* gum/poly(vinyl alcohol) hydrogels as a superabsorbent. ACS Omega 5(29):17955–17961. https://doi.org/10.1021/acsomega.0c01023
37. Mahdi S, Mirzadeh H, Zandi M, Barzin J (2017) Designing and fabrication of curcumin loaded PCL/PVA multi-layer nanofibrous electrospun structures as active wound dressing. Prog Biomat 6(1–2):39–48. https://doi.org/10.1007/s40204-017-0062-1
38. Sibusiso A, Xhamla N, Blessing AA (2020) Polymer based materials loaded with curcumin for wound healing applications. Polymers 12:2286. https://doi.org/10.3390/polym12102286
39. Capella V, Rivero RE, Liaudat AC, Ibarra LE, Roma DA, Alustiza F, Mañas F, Barbero P, Bosch CA, Rivarola R, Rodriguez N (2019) Cytotoxicity and bioadhesive properties of poly-N-isopropylacrylamide hydrogel. Heliyon 5(4):e01474. https://doi.org/10.1016/j.heliyon.2019.e01474
40. Jayaraj S, Parthasarathy V, Mahalakshmi S, Anbarasan R, Kumar PS, Daramola MO (2019) Enhancement in thermal, mechanical and electrical properties of novel PVA nanocomposite embedded with SrO nanofillers and the analysis of its thermal degradation behavior by nonisothermal approach. Polym Compos 3:1–14. https://doi.org/10.1002/pc.25453
41. Selvi J, Parthasarathy V, Mahalakshmi S, Anbarasan R, Daramola MO, Senthil Kumar P (2020) Optical, electrical, mechanical, and thermal properties and non-isothermal decomposition behavior of poly(vinyl alcohol)–ZnO nanocomposites. Iran Polym J 29:411–422. https://doi.org/10.1007/s13726-020-00806-8
42. Wang Z, Ding Y, Wang J (2019) Novel polyvinyl alcohol (PVA)/cellulose nanocrystal (CNC) supramolecular composite hydrogels: preparation and application as soil conditioners. Nanomat 9:1397. https://doi.org/10.3390/nano9101397
43. Siddaiah T, Ojha P, Gopal NO, Kumar VR (2018) Structural, optical and thermal characterizations of PVA/MAA:EA polyblend films. Mat Res 21(5). https://doi.org/10.1590/1980-5373-mr-2017-0987
44. Solanga Alvarez G, Helary C, MathildeMebert A, Wang X, Coradin T, Federico Desimone M (2014) Antibiotic – loaded silica nanoparticle - collagen composite hydrogels with prolonged antimicrobial activity for wound infection prevention. J Mater Chem B 2:4660
45. Bukhari SMH, Khan S, Rehanullah M, Ranjha NM (2015) Synthesis and characterization of chemically cross-linked acrylic acid/gelatin hydrogels: effect of pH and composition on swelling and drug release. Inter J Polym Sci Article ID 187961.https://doi.org/10.1155/2015/187961
46. Muhammad UAK, Saiful IAR, Hassan M, Rehman S, Wafa SAA, Rashid A (2021) Antibacterial and hemocompatible pH-responsive hydrogel for skin wound healing application: *Invitro* drug release. Polymers 13:3703
47. Samina N, Muhammad U, Wafa S, Saiful I, Aneela J, Mohammed R (2021) Nanocomposite hydrogels for melanoma skin cancer care and treatment: in-vitro drug delivery, drug release kinetics and anti-cancer activities. Arab J Chem 14:103120